New insights into transformation mechanisms for sulfate and chlorine radical-mediated degradation of sulfonamide and fluoroquinolone antibiotics

Jinshuai Zheng[a], Junfeng Niu[b], Crispin Halsall[c], Xiaojia Che[a], Peng Zhang[a], Linke Ge[a,c,*]

[a] School of Environmental Science and Engineering, Shaanxi University of Science & Technology, Xi'an 710021, P. R. China
[b] College of Environmental Science and Engineering, North China Electric Power University, Beijing, 102206, P. R. China
[c] Lancaster Environment Centre, Lancaster University, Lancaster LA1 4YQ, United Kingdom

ARTICLE INFO

Article history:
Received
Received in revised form
Accepted
Available online

Keywords:
Antibiotics
Dissociation
Degradation kinetics
Reactive species
Transformation pathways
Risks

ABSTRACT

As antibiotic pollutants cannot be incompletely removed by conventional wastewater treatment plants, ultraviolet (UV) based advanced oxidation processes (AOPs) such as UV/persulfate (UV/PS) and UV/chlorine are increasing concerned for the effective removal of antibiotics from wastewaters. However, the specific mechanisms involving the degradation kinetics and transformation mechanisms are not well elucidated. Here we report a detailed examination of $SO_4^{\bullet-}$/Cl•-mediated degradation kinetics, products and toxicities of sulfathiazole (ST), sarafloxacin (SAR) and lomefloxacin (LOM) in the two processes. Both $SO_4^{\bullet-}$/Cl•-mediated transformation kinetics were found to be dependent on pH ($p < 0.05$), which was attributed to the disparate reactivities of their individual dissociation forms. Based on competition kinetic experiments and matrix calculations, the cationic forms (H_2ST^+, H_2SAR^+ and H_2LOM^+) were more highly reactive towards $SO_4^{\bullet-}$ in most cases, while the neutral forms (e.g., $HSAR^0$ and $HLOM^0$) reacted the fastest with Cl• for the most of the antibiotics tested. Based on the identification of 31 key intermediates using tandem mass spectrometry, those reactions generated different products, of which the majority still retained the core chemical structure of the parent compounds. The corresponding diverse transformation pathways were proposed, involving S−N breaking, hydroxylation, defluorination and chlorination reactions. Furthermore, toxicity changes of their reaction solutions as well as the toxicity of each intermediate were evaluated by *vibrio fischeri* and ECOSAR model, respectively. Many primary by-products were proved to be more toxic than the parent chemical, raising the wider issue of extended potency for these compounds with regards to their ecotoxicity. These results have implications when assessing the degradative fate and risk of these chemicals during the AOPs that are increasingly used in tertiary wastewater treatment processes.

Antibiotics, as a class of emerging contaminants, have become an environmental topic of acute concern due to their pseudo-persistence and ecological risk in aquatic systems [1-3]. As necessities, antibiotics are widely used in human treatments, animal husbandry and aquaculture [4-6]. Then, they are mainly released from hospitals and households into wastewater treatment plants (WWTPs) [7, 8]. However, most antibiotics cannot be incompletely removed by conventional wastewater treatment processes and are therefore frequently discharged into the aquatic environment [9, 10]. Their aqueous ubiquity in surface waters has been reported in many countries, including Europe, the United States, and China [11-13]. Even trace amounts of antibiotics persisting in the aquatic environment can have long-term adverse effects [14]. Antibiotic pollutants are resistant to biodegradation in the environment, but their presence in freshwater systems induces the generation of antibiotic resistant bacteria and poses a threat to ecosystem and human health [15]. Therefore, it is necessary to control such pollutants in wastewater to prevent them from entering the aquatic environment.

Conventional wastewater treatment processes including adsorption, sedimentation and biodegradation cannot remove antibiotics effectively [16-18]. Ultraviolet (UV) based advanced oxidation processes (AOPs) have been reported to effectively degrade antibiotics [6, 19, 20]. UV/persulfate (UV/PS) and UV/chlorine have received increasing attention in the degradation of antibiotics in wastewater because of their strong oxidation ability, high efficiency, and limited secondary pollution [21-23]. Many previous studies have investigated influencing factors of the UV/PS and UV/chlorine processes [24-27], and the pH values of the reaction system were found to significantly affect the degradation efficiency of some certain pollutants [28, 29]. For instance, although the degradation of sulfachloropyridazine in the UV/PS process at different pH conditions followed pseudo-first-order reaction kinetics, the fastest reaction rate appeared at pH = 5 [30]. Yang et al. [31] observed the fastest degradation of ciprofloxacin (CIP) at pH = 7 and pH = 5, respectively in the UV/PS and UV/chlorine processes, and deduced that the phenomena might be attributed to the diverse reactivities of CIP toward reactive species at different pH. As the molecular structures contain ionizable groups (e.g., −COOH and $-NH_n$), most antibiotics are ionizable and will undergo acid-base dissociation, exhibiting different dissociated species depending on the pH of the water [32-34]. These dissociated species have been proved to have unique physicochemical properties [34]. As for the UV/PS and UV/chlorine processes, previous studies have found that pH had a significant effect on the degradation of ionizable antibiotics by $SO_4^{\bullet-}$ and Cl•, but the specific mechanisms involving the degradation kinetics and transformation products are not well elucidated [23, 27, 31]. Therefore, it is necessary to clarify the degradation behavior and related mechanisms of antibiotics in different dissociated forms in the two processes.

* Corresponding author.
E-mail address: gelinke@sust.edu.cn (L. Ge).

This study provides a detailed examination of $SO_4^{\bullet-}$/Cl•-mediated degradation of sulfathiazole (ST), sarafloxacin (SAR) and lomefloxacin (LOM) in UV/PS and UV/chlorine systems. The experiments were carried out using a merry-go-round photochemical reactor (Fig. S1). ST, SAR and LOM (purity > 98%) were purchased from J&K. Their chemical structures and molecular weights are shown in Table S1. In the competition kinetics experiments, $Na_2S_2O_8$ (40 μM) and NaClO (40 μM) were used to generate $SO_4^{\bullet-}$ and Cl•, respectively. The initial concentrations of the antibiotic pollutants were set at 5 μM. The bimolecular reaction rate constants $k_{ROS,S}$ ($k_{SO4\bullet-,S}$ and $k_{Cl\bullet,S}$) for the three model substances (S) with $SO_4^{\bullet-}$ and Cl• were calculated by equations 1−4 [33, 35],

$$k_{ROS,S} = \frac{\ln([S]_t/[S]_0)}{\ln([R]_t/[R]_0)} k_{ROS,R} \quad (1)$$

$$[\bullet OH]_{SS} = \frac{k_{NB}}{k_{\bullet OH,NB}} \quad (2)$$

$$[Cl\bullet]_{SS} = \frac{k_{BA} - \left[\frac{k_{\bullet OH,BA}}{k_{\bullet OH,NB}}\right] k_{NB}}{k_{Cl\bullet,BA}} \quad (3)$$

$$k_{Cl\bullet,S} = \frac{k_S - k_{\bullet OH,S}[\bullet OH]_{SS}}{[Cl\bullet]_{SS}} \quad (4)$$

where $k_{ROS,R}$ denotes the bimolecular reaction rate constants of the references (R), $k_{SO4\bullet-,BA} = 1.2 \times 10^9\ M^{-1}\ s^{-1}$, $k_{Cl\bullet,BA} = 1.8 \times 10^{10}\ M^{-1}\ s^{-1}$, $k_{\bullet OH,BA} = 5.9 \times 10^9\ M^{-1}\ s^{-1}$, $k_{\bullet OH,NB} = 3.9 \times 10^9\ M^{-1}\ s^{-1}$; $[\bullet OH]_{SS}$ and $[Cl\bullet]_{SS}$ represent the steady-state concentrations of •OH and Cl•, respectively. *Vibrio fischeri* was selected to examine the 15-minute acute toxicities of the samples during degradation processes according to the international standard method (ISO11348-3-2007). The experimental information is detailed in the supporting information.

In all control experiments, no significant degradation of ST, SAR and LOM was observed ($p > 0.1$), suggesting that their pyrolysis and hydrolysis were negligible. As shown in Fig. S2, these model compounds had no light absorption at $\lambda > 420$ nm, and thus did not undergo direct photolysis (< 2%). When exposed to light irradiation ($\lambda > 420$ nm), all the three compounds disappeared rapidly in the competition kinetics experiments, indicating that they were effectively degraded by $SO_4^{\bullet-}$/Cl•. It can be seen from the degradation curves in Fig. 1 that the apparent reactions of the three individual substances with the reactive species were conformed to follow pseudo-first-order kinetics ($R^2 > 0.95$), depending on the pH. However, the degradation of the substances by the reactive species ($SO_4^{\bullet-}$/Cl•) were essentially second-order bimolecular reactions. Thus, the calculated values for the bimolecular reaction rate constants ($k_{SO4\bullet-,S}$ and $k_{Cl\bullet,S}$) are shown in Table S2. The $k_{SO4\bullet-,S}$ ranged from $(1.80 \pm 0.05) \times 10^9\ M^{-1}\ s^{-1}$ for ST (pH = 8) to $(8.73 \pm 0.33) \times 10^{10}\ M^{-1}\ s^{-1}$ for LOM (pH = 10), while $k_{Cl\bullet,S}$ ranged from $(3.44 \pm 0.23) \times 10^9\ M^{-1}\ s^{-1}$ for SAR (pH = 10) to $(3.31 \pm 0.002) \times 10^{11}\ M^{-1}\ s^{-1}$ for LOM (pH = 8).

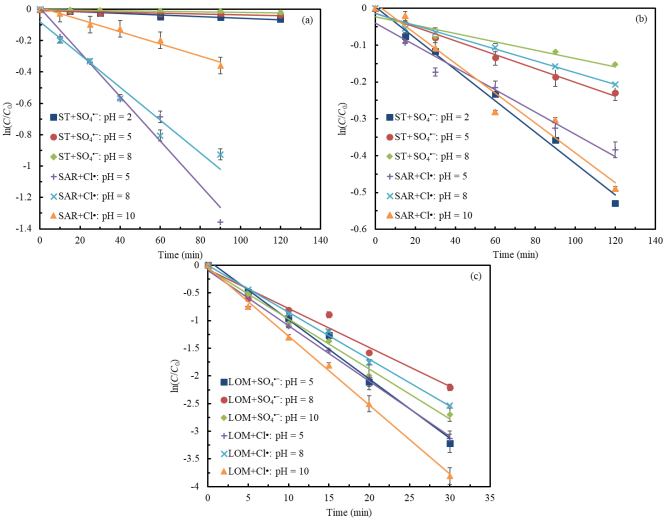

Fig. 1. Kinetic profiles for the reactions of sulfathiazole (ST), sarafloxacin (SAR) and lomefloxacin (LOM) with $SO_4^{\bullet-}$/Cl• under different pH conditions

As shown in Fig. 2a, both $k_{SO4\bullet-,S}$ and $k_{Cl\bullet,S}$ of each compound were dependent on pH ($p < 0.05$). As for ST, $k_{SO4\bullet-,ST}$ and $k_{Cl\bullet,ST}$ were slightly higher at pH = 2 than at pH = 5 and 8. However, $k_{SO4\bullet-,S}$ was maximum at pH = 5 for SAR reacting with $SO_4^{\bullet-}$, while LOM was the most reactive toward $SO_4^{\bullet-}$ at pH = 10. In addition, both the $k_{Cl\bullet,S}$ values of SAR and LOM were greatest when reacting with Cl• at pH = 8. The pH dependence of the reactivities in UV/PS and UV/chlorine reactions was caused by Coulomb's force and chemical structures. The coulombic repulsion between reactants under alkaline conditions leads to lower reactivities [36]. Meanwhile, the molecular structures and deprotonation degrees might have impacts on the pH dependence [33, 37], indicating that the ROS oxidative reactivities of various dissociation forms of these ionizable antibiotics need to be further differentiated.

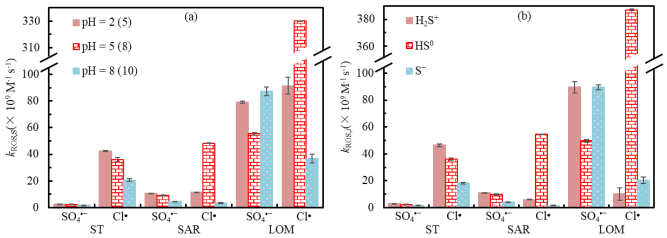

Fig. 2. The bimolecular reaction rate constants of sulfathiazole (ST), sarafloxacin (SAR) and lomefloxacin (LOM) with $SO_4^{\bullet-}$/Cl• (a is for different pH conditions, b is for different dissociation forms. S represents the model substances)

To quantify the reactivities of each protonated form towards $SO_4^{\bullet-}$ and Cl•, the bimolecular reaction rate constants ($k_{SO4\bullet-,i}$, $k_{Cl\bullet,i}$) of different dissociation forms (i) were obtained by matrix calculations, and the results are shown in Fig. 2b (detailed data listed in Table S3). The various dissociation forms of the individual antibiotics exhibited different reactivities (from H_2ST^+ to ST^-; H_2FQs^+ to FQs^-). For ST, the cationic forms (H_2ST^+) were more reactive toward $SO_4^{\bullet-}$ and Cl•. The cationic SAR (H_2SAR^+) had highest reactivity towards $SO_4^{\bullet-}$, while the anionic and cationic LOM (LOM^- and H_2LOM^+) was more reactive with $SO_4^{\bullet-}$. Interestingly, both SAR and LOM in the neutral forms ($HFQs^0$) showed the fastest reactions when reacting with Cl•. Compared with the $SO_4^{\bullet-}$ mediated reaction, the reactivities of FQs toward Cl• varied by 3 orders of magnitude based on the profile (pH = 8 or 10).

As the pHincreases , the dissociated forms gradually changed (Fig. S3), which can explain why the oxidation reactivities were significantly related to pH (Fig. 2). Overall, the cationic forms (H_2ST^+, H_2SAR^+ and H_2LOM^+) were more highly reactive towards $SO_4^{\bullet-}$ in most cases, while the neutral forms (e.g., $HSAR^0$ and $HLOM^0$) reacted the fastest with Cl• for the most of the antibiotics tested.

Furthermore, we identified 31 significant intermediates generated from $SO_4^{\bullet-}$/Cl•-mediated degradation of the three antibiotics in the UV/PS and UV/chlorine processes. The proposed chemical structures and tentative transformation pathways are presented in Figs. 3−5. Table S4 shows detailed information about these degradation products, including retention times (t_R), molecular weights (M_w), and MS fragment *m*/*z*. The total ion chromatograms and MS spectra in positive ionization mode are shown in Figs. S4 and S5. There are different intermediates and transformation pathways corresponding to the two reactions of the individual antibiotics (Figs. 3−5). As for ST (Fig. 3), the transformation products of the reaction with $SO_4^{\bullet-}$ were simple, mainly because $SO_4^{\bullet-}$ was easy to selectively attack electron-rich groups like anilines [38], resulting in the S−N breaking and the formation of P155 and P100. The products were also detected for the photolysis of ST [39]. In contrast, the primary products in the reaction process of ST with Cl• were abundant, with more reaction pathways involving five-membered heterocyclic ring opening, hydroxylation, and dealkylation. This could be attributed to the diversity of reactive species (Cl• and •OH) in the UV/chlorine process [40]. The •OH preferred to experience multi-site oxidation with phenyl hydroxylation and heterocyclic cleavage [33], while Cl• was easy to attack single bonds and amino groups [21, 41]. Therefore, the five-membered heterocycles in the ST structure were easily to be cleaved.

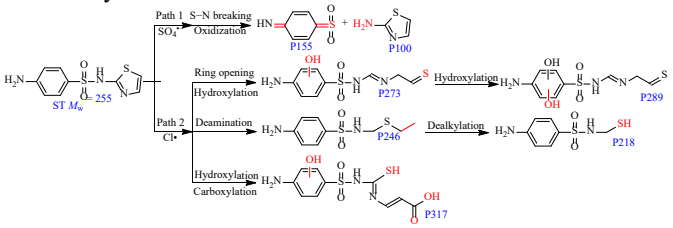

Fig. 3. Primary transformation products and pathways of sulfathiazole (ST) during UV/PS and UV/chlorine processes. The products are labeled "P*n*", with *n* standing for the molecular weights

For SAR (Fig. 4), the same transformation products, P359 and P383, were observed in both UV/PS and UV/chlorine processes. This is mainly due to the susceptibility of SAR's piperazine ring and −F group to be attacked by the reactive species, resulting in ring opening and defluorination reactions [42]. Meanwhile, there were different degradation products (P232, P351, and P381, etc.) generated during the two processes because of the different oxidation capacity and attack sites of $SO_4^{\bullet-}$ and Cl•. Based on the transformation products of SAR, then primary reaction pathways were proposed. These included: defluorination; hydroxylation; and piperazinyl cleavage. Importantly, SAR underwent chlorination during the UV/chlorine process, indicating the participation of Cl• in the reaction. The chlorinated product (P351) is of concern due to its complex biological effects [43-45]. Compared with SAR, the more degradation products (P273, P331, and P349) of LOM (Fig. 5) were similar for UV/PS and UV/chlorine processes, mainly because LOM had more alkane structures and was susceptible to attack by $SO_4^{\bullet-}$ and Cl• [38]. Based on these transformation products, the proposed primary pathways of LOM are defluorination, piperazinyl ring opening, hydroxylation, et al.

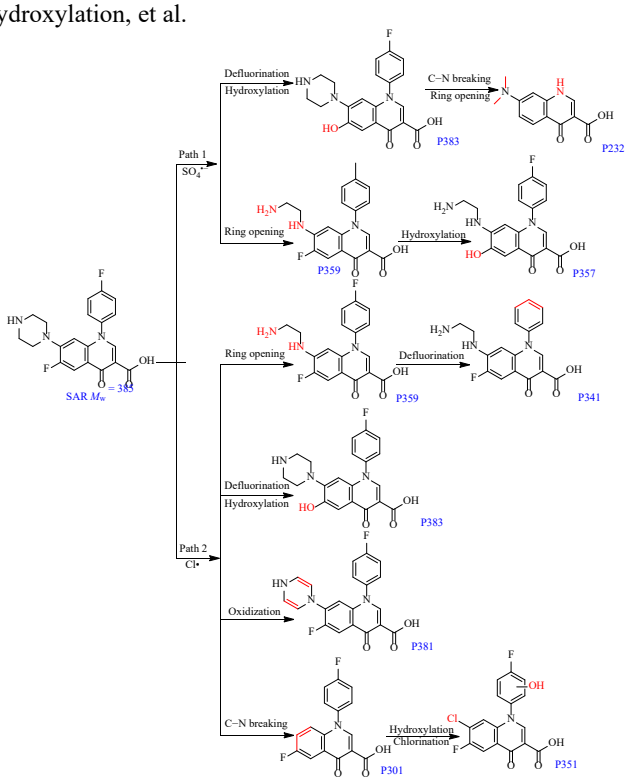

Fig. 4. Products and primary pathways of sarafloxacin (SAR) reacting with $SO_4^{\bullet-}$/Cl•

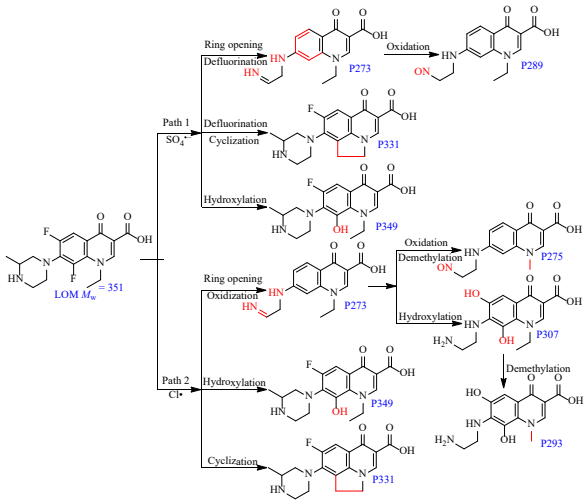

Fig. 5. Transformation products and primary pathways of lomefloxacin (LOM) during UV/PS and UV/chlorine processes

The toxicity of the 3 target antibiotics during the $SO_4^{\bullet-}$/Cl• mediated degradation processes was assayed, for which the results are shown in Fig. 6. There are certain similarities and differences in the toxicity changes for the individual antibiotics towards the two reactive species. For ST, the toxicities of the both reaction systems firstly increased, and then decreased with the time, implying the generation of some more toxic intermediates than the parent compound. However, toxicities for the Cl• mediated reaction solution of ST were more enhanced at the initial period ($0-t_{1/2}$) of degradation, which can be attributed to the abundant intermediates that contain the basic parent structure (Fig. 3).

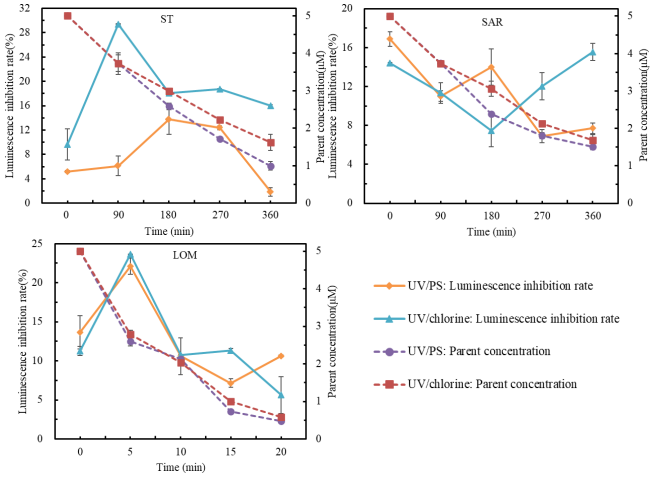

Fig. 6. Concentration changes and solution luminescence inhibition rates of sulfathiazole (ST), sarafloxacin (SAR), and lomefloxacin (LOM) during UV/PS and UV/chlorine processes

As for SAR and LOM, their toxicity profilewas diverse, not only for the two reaction systems, but also for the different FQs (Fig. 6). The toxicities observed during the reaction of SAR with $SO_4^{\bullet-}$ showed an overall decreasing trend with time, while the toxicities were initially reduced and then enhanced during the reaction between SAR and Cl•. Unlike SAR, the toxicity trends of LOM during the reaction with $SO_4^{\bullet-}$ and Cl• were similar, which may be due to the formation of similar transformation products (Fig. 5).

The observed toxicity profile wasrelated to the formation and accumulation of transformation products, of which some would be more toxic and others less toxic than the parent compounds. The toxicities of these individual intermediates were assessed using ECOSAR v2.0 software, with their 96 h LC_{50} (fish), 48 h LC_{50} (daphnia) and 96 h EC_{50} values (green algae) shown in Table S5. It can be found that ST, SAR and LOM all generated intermediates with higher toxicities than the parents during the degradation processes, such as the transformation products P100, P218 and P246 for ST, P301, P351, P357 and P383 for SAR, as well as P275 and P289 for LOM. These were consistent with the results of *vibrio fischeri* toxicity experiments, implying that the toxicities of the reaction systems would persist in these initial intermediates. Therefore, ecological risks of the treated antibiotic wastewaters by the UV/PS and UV/chlorine processes need to be considered before treated-wastewater release into the aquatic environment.

In summary, this study provides new insights into the $SO_4^{\bullet-}$/Cl•-mediated degradation kinetics, products, toxicities, and related mechanisms of the three representative antibiotics in UV/PS and UV/chlorine processes. The transformation kinetics were found to be dependent on pH ($p < 0.05$), which was attributable to the disparate reactivities of their individual dissociated forms when reacting with reactive species (e.g. $SO_4^{\bullet-}$ and Cl•). These reactions generated different products, and demonstrated diverse transformation pathways, involving S–N cleavage , hydroxylation, defluorination and chlorination reactions. This has implications when assessing the degradative fate of these chemicals during the AOPs that are increasingly used in tertiary wastewater treatment processes.

Furthermore, we find that many primary by-products exhibited similar structures to the parent compounds and revealed atoxicity profile of ST, SAR and LOM reaction systems before and after degradation. The toxicity responses were dependent on the major intermediates and primary pathways. Many intermediates were proved to be more toxic than their individual parents, raising the wider issue of extended potency for these compounds with regards to their ecotoxicity. These results provide novel knowledge for understanding the UV-based AOPs to treat wastewater containing antibiotics.

Declaration of competing interest

The authors declare that they have no known competing financial interests or personal relationships that could have appeared to influence the work reported in this paper.

Acknowledgments

This work was supported by the Key Research and Development Program of Shaanxi Province (No. 2024SF-YBXM-567), the National Natural Science Foundation of China (No. 21976045, 22076112), and the China Scholarship Council (CSC) Scholarship (No. 202308610123).

References

[1] E. Brillas, Sci. Total Environ., 819 (2022) 153102.
[2] K. Brooks, J. Eze, O. Onalenna, T.O. Rahube, J. Hazard. Mater. Adv., 9 (2023) 100232.
[3] H. Malik, R. Singh, S. Kaur, P. Dhaka, J.S. Bedi, J.P.S. Gill, G. Gongal, J. Infect. Public Health, 16 (2023) 172-182.
[4] J. Ren, H. Shi, J. Liu, C. Zheng, G. Lu, S. Hao, Y. Jin, C. He, J. Environ. Manage., 335 (2023) 117546.
[5] X. Wang, J. Jing, M. Zhou, R. Dewil, Chin. Chem. Lett., 34 (2023) 107621.
[6] R. Guo, Y. Chen, B. Liu, Y. Han, J. Gou, X. Cheng, Chin. Chem. Lett., 33 (2022) 3809-3817.
[7] F. Yan, L. An, X. Xu, W. Du, R. Dai, Sci. Total Environ., 906 (2024) 167737.
[8] C. Zhang, Y. Chen, S. Chen, X. Guan, Y. Zhong, Q. Yang, Ecotoxicol. Environ. Saf., 255 (2023) 114817.
[9] J. Wang, R. Zhuan, L. Chu, Sci. Total Environ., 646 (2019) 1385-1397.
[10] Y. Pan, Y. Zhang, M. Zhou, J. Cai, Y. Tian, Water Res., 153 (2019) 144-159.
[11] C.E. Givens, D.W. Kolpin, L.E. Hubbard, S.M. Meppelink, D.M. Cwiertny, D.A. Thompson, R.F. Lane, M.C. Wilson, Sci. Total Environ., 904 (2023) 166753.
[12] D. Han, Q. Hou, J. Song, R. Liu, Y. Qian, G. Huang, Environ. Res., 235 (2023) 116653.
[13] U. Szymańska, M. Wiergowski, I. Sołtyszewski, J. Kuzemko, G. Wiergowska, M.K. Woźniak, Microchem. J., 147 (2019) 729-740.
[14] G. Liu, H. Zheng, J. Lu, Trends Environ. Anal. Chem., 16 (2017) 16-23.
[15] N. Guo, Y. Wang, L. Yan, X. Wang, M. Wang, H. Xu, S. Wang, Water Res., 117 (2017) 95-101.
[16] J. Dutta, A.A. Mala, Water Sci. Technol., 82 (2020) 401-426.
[17] A.C. Reis, B.A. Kolvenbach, O.C. Nunes, P.F. Corvini, New Biotechnol., 54 (2020) 34-51.
[18] D. Zhi, D. Yang, Y. Zheng, Y. Yang, Y. He, L. Luo, Y. Zhou, J. Environ. Manage., 251 (2019) 109598.
[19] Z. Li, J. Wang, J. Chang, B. Fu, H. Wang, Sci. Total Environ., (2022) 159172.
[20] J. Liu, H. He, Z. Shen, H.H. Wang, W. Li, J. Hazard. Mater., 429 (2022) 128398.

[21] N. Li, J. Ye, H. Dai, P. Shao, L. Liang, L. Kong, B. Yan, G. Chen, X. Duan, Water Res., 235 (2023) 119926.
[22] Z. Li, L. Wang, Y. Liu, P. He, X. Zhang, J. Chen, H. Gu, H. Zhang, J. Ma, Water Res., 195 (2021) 116973.
[23] Y. Zhang, L. Li, Z. Pan, Y. Zhu, Y. Shao, Y. Wang, K. Yu, Chem. Eng. J., 379 (2020) 122354.
[24] E. Bazrafshan, P. Tavassoli, A.A. Zarei, Water Sci. Technol., 2017 (2018) 126-133.
[25] N. Huang, W. Wang, Z. Xu, Q. Wu, H. Hu, J. Environ. Manage., 237 (2019) 180-186.
[26] M.Y. Kilic, W.H. Abdelraheem, X. He, K. Kestioglu, D.D. Dionysiou, J. Hazard. Mater., 367 (2019) 734-742.
[27] Y. Zhang, J. Zhang, Y. Xiao, V.W.C. Chang, T.-T. Lim, Chem. Eng. J., 302 (2016) 526-534.
[28] M. Xu, J. Deng, A. Cai, C. Ye, X. Ma, Q. Li, S. Zhou, X. Li, Chem. Eng. J., 413 (2021) 127533.
[29] Z. Xu, C. Shan, B. Xie, Y. Liu, B. Pan, Appl. Catal., B, 200 (2017) 439-447.
[30] J. Dan, Q. Wang, K. Mu, P. Rao, L. Dong, X. Zhang, Z. He, N. Gao, J. Wang, Environ. Sci. Water Res. Technol., 6 (2020) 2510-2520.
[31] H. Yang, Y. Li, Y. Chen, G. Ye, X. Sun, Water Environ. Res., 91 (2019) 1576-1588.
[32] L. Ge, Q. Dong, C. Halsall, C.-E. Chen, J. Li, D. Wang, P. Zhang, Z. Yao, Environ. Sci. Pollut. Res., 25 (2018) 15726-15732.
[33] L. Ge, P. Zhang, C. Halsall, Y. Li, C. Chen, J. Li, H. Sun, Z. Yao, Water Res., 149 (2019) 243-250.
[34] X. Wei, J. Chen, Q. Xie, S. Zhang, L. Ge, X. Qiao, Environ. Sci. Technol., 47 (2013) 4284-4290.
[35] J. Fang, Y. Fu, C. Shang, Environ. Sci. Technol., 48 (2014) 1859-1868.
[36] X. Tong, S. Wang, L. Wang, Chemosphere., 256 (2020) 126997.
[37] T. Mill, Chemosphere., 38 (1999) 1379-1390.
[38] X. Li, J. Shen, H. Cao, W. Zhang, Z. Sun, F. Ma, Q. Gu, Chem. Eng. J., 474 (2023) 146256.
[39] A.L. Boreen, W.A. Arnold, K. McNeill, Environ. Sci. Technol., 38 (2004) 3933-3940.
[40] T.-K. Kim, T. Kim, Y. Cha, K.-D. Zoh, Water Res., 185 (2020) 116159.
[41] Y. Lei, S. Cheng, N. Luo, X. Yang, T. An, Environ. Sci. Technol., 53 (2019) 11170-11182.
[42] N. Li, R. Li, X. Duan, B. Yan, W. Liu, Z. Cheng, G. Chen, L.-a. Hou, S. Wang, Environ. Sci. Technol., 55 (2021) 16163-16174.
[43] S. Kali, M. Khan, M.S. Ghaffar, S. Rasheed, A. Waseem, M.M. Iqbal, M. Bilal khan Niazi, M.I. Zafar, Environ. Pollut., 281 (2021) 116950.
[44] B.T. Oba, X. Zheng, M.A. Aborisade, A.Y. Battamo, A. Kumar, S. Kavwenje, J. Liu, P. Sun, Y. Yang, L. Zhao, Environ. Pollut., 291 (2021) 118239.
[45] A. Riu, A. le Maire, M. Grimaldi, M. Audebert, A. Hillenweck, W. Bourguet, P. Balaguer, D. Zalko, Toxicol. Sci., 122 (2011) 372-382.